Ideal Glass States Are Not Purely Vibrational: Insight from Randomly Pinned Glasses

Misaki Ozawa,[1] Atsushi Ikeda,[2] Kunimasa Miyazaki,[3] and Walter Kob[1,*]
[1]Laboratoire Charles Coulomb (L2C), University of Montpellier and CNRS, F-34095 Montpellier, France
[2]Graduate School of Arts and Sciences, University of Tokyo, Tokyo 3–8–1, Japan
[3]Department of Physics, Nagoya University, Nagoya 464-8602, Japan

(Received 5 April 2018; published 14 November 2018)

We use computer simulations to probe the thermodynamic and dynamic properties of a glass former that undergoes an ideal glass transition because of the presence of randomly pinned particles. We find that even deep in the equilibrium glass state, the system relaxes to some extent because of the presence of localized excitations that allow the system to access different inherent structures, thus giving rise to a nontrivial contribution to the entropy. By calculating with high accuracy the vibrational part of the entropy, we show that also in the equilibrium glass state thermodynamics and dynamics give a coherent picture, and that glasses should not be seen as a disordered solid in which the particles undergo just vibrational motion but instead as a system with a highly nonlinear internal dynamics.

DOI: 10.1103/PhysRevLett.121.205501

The nature of the glass transition is one of the most challenging research topics in condensed matter physics and has therefore been the focus of a multitude of studies [1–5]. Many aspects of the slow and complex dynamics of supercooled liquids and the resulting glass transition have been successfully explained in terms of the potential energy landscape (PEL) [6–10]. In this framework, the configurational space of the system is partitioned into basins of attraction of the local energy minima (the inherent structures, ISs) of the potential energy, and the dynamics at low temperatures is characterized as the motion through the complex pathway that connects neighboring basins. The conventional description of glasses is that the glass state corresponds to a vibrational motion around the ISs, which in real space means that the particles are trapped by the cages formed by their neighbors and vibrate around a fixed amorphous configuration. However, recent experiments challenge this view, since they seem to suggest that certain types of relaxation processes are present even in the glass, implying that the motion of the atoms is more complex than pure vibrations [11–13]. However, it is difficult to decide whether these relaxation processes are indeed an equilibrium property of the sample or just related to aging. The existence of equilibrium relaxation processes in the glass state implies that even at low temperatures the system explores a complex landscape; i.e., it can access in a *finite* time many different local minima. This in turn has the consequence that the conventional definition of the configurational entropy s_{conf} as the difference between the total entropy s_{tot} of the system and its purely vibrational part s_{vib} should be questioned. Thus, the study of (equilibrium) relaxation processes in the equilibrium glass state will allow us to advance our understanding of the meaning of the glass state on the microscopic level.

Advancing on this question has so far been hampered by the fact that it was impossible to generate equilibrium glasses (also called "ideal glasses"), i.e., *equilibrium* structures at very low temperatures. This situation has recently changed since it has been realized that if one pins (immobilizes) randomly a finite fraction c of the particles [14], the fluid particles, i.e., nonpinned ones, undergo an equilibrium glass transition if c is increased beyond a certain threshold [15,16]. Numerical simulations of simple glass formers have confirmed that this pinning approach does indeed allow us to observe an equilibrium glass transition at which the entropy shows a marked bend, and hence to access the equilibrium glass state [17,18]. Thus, these results have opened the door to studying the properties of equilibrium glasses, and in the following we will demonstrate that even in the ideal glass state relaxation processes are present, implying that in the glass the entropy is not just given by the vibrational contribution.

We simulate a binary mixture of N Lennard-Jones (LJ) particles in three dimensions [19], of which a fraction c are permanently pinned. N is 300 or 1200, and we use the standard LJ units for the length, energy, and temperature, setting the Boltzmann constant $k_B = 1$. First, we have equilibrated the system without pinned particles at a given temperature T, then the positions of cN particles are frozen, and we study the static and dynamical properties of the remaining $(1-c)N$ nonpinned particles of the system. To study the static properties, we use the parallel tempering (PT) molecular dynamics method with 24 replicas [20,21] (see Refs. [17,18] for details on the pinning procedure and the PT). For the dynamical properties we use the standard Monte Carlo (MC) dynamics simulation [22], where an elementary move is a random displacement of a randomly chosen particle within a linear box of size $\delta = 0.15$.

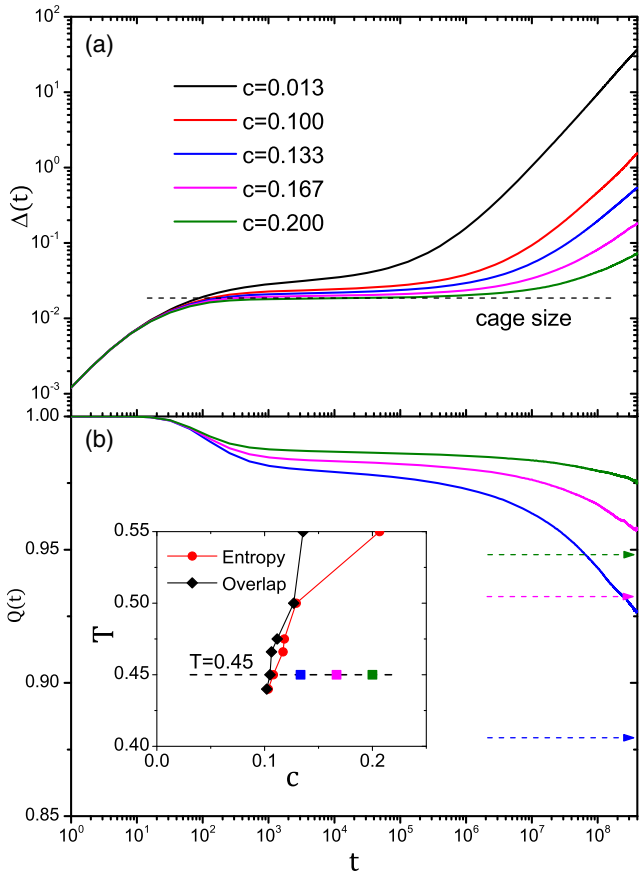

FIG. 1. (a) Time dependence of the mean squared displacement $\Delta(t)$ for different concentrations of pinned particles, c, at $T = 0.45$ for $N = 1200$. The horizontal dashed line is the height of the plateau for $c = 0.2$. (b) The dynamic overlap function $Q(t)$ at $T = 0.45$ for $N = 1200$ and concentrations c at which the system is in the equilibrium glass state. The horizontal dashed arrows are the static overlap functions $Q^{(\mathrm{static})}$ evaluated from the parallel tempering simulations. The inset shows the state points for the presented $Q(t)$ in the phase diagram from Ref. [18].

One MC step, which is our unit of time, consists of $(1-c)N$ such attempts. Despite the huge acceleration of the sampling due to the PT, we found that runs up to 2×10^{10} steps were needed to get statistically significant results. This, and the necessary averaging over the independent realizations of the pinned configurations (typically 25 for $N = 300$ and 10 for $N = 1200$) required about 150 years of CPU time.

To probe the relaxation dynamics of the system, we focus on $T = 0.45$ and increase c, thus crossing at around $c = 0.1$ the boundary between fluid and glass state [see inset of Fig. 1(b)]. Figure 1(a) shows the mean squared displacement (MSD) for different values of c: $\Delta(t) = \sum_{i=1}^{(1-c)N}[\langle|\mathbf{r}_i(t) - \mathbf{r}_i(0)|^2\rangle]/(1-c)N$. Here $\langle\cdots\rangle$ and $[\cdots]$ are the thermal and disorder averages, respectively. Note that we have averaged the MSD over both species of particles. At intermediate times $\Delta(t)$ has a marked plateau that is related to the usual cage effect observed in glassy systems [1], and the horizontal dashed line indicates the plateau height of $\Delta(t)$ at $c = 0.2$. Surprisingly, we find that even in the equilibrium glass phase, i.e., at this temperature for $c \geq 0.1$ (see the Supplemental Material [23]), $\Delta(t)$ shows at long times a marked increase above this plateau, indicating that the particles can leave their cage. To understand this behavior, we analyze the van Hove correlation function [23] and find that the particles undergo an exchange motion, i.e., the particles tend to be replaced by the same kind of particles (see the Supplemental Material [23]). This seems to explain the upturn of the mean squared displacement. More surprising are the results regarding the collective overlap $Q(t) = \sum_{i,j}[\langle\theta(a - |\mathbf{r}_i(t) - \mathbf{r}_j(0)|)\rangle]$, where $\theta(x)$ is the Heaviside function and $a = 0.3$. This function probes the *collective* relaxation of the system and is not affected by the particle exchange motions. Figure 1(b) shows that $Q(t)$ decays slightly after the plateau at intermediate times, before it decays to its long-time limit [horizontal dashed lines $Q(t \to \infty) = Q^{(\mathrm{static})}$], a quantity that can be calculated with high accuracy directly from the PT simulations. The very high value of $Q^{(\mathrm{static})} > 0.85$ and the strong c dependence of this quantity, see Ref. [18], demonstrates that the explored state points are indeed glass states, and hence we can conclude that the system shows a subtle and nontrivial relaxation dynamics even in the ideal glass. In the Supplemental Material we show that this is *not* an out-of-equilibrium effect [23].

The presence of this relaxation dynamics is at odds with the results of Ref. [18] that in the glass phase the configurational entropy s_{conf} seems to be zero [see red circles in Fig. 3(b)], since $s_{\mathrm{conf}} = 0$ implies that there are no states into which the system can move to relax. In that work s_{conf} was estimated from $s_{\mathrm{tot}} - s_{\mathrm{harm}}$, where s_{harm} is the entropy of the strictly harmonic solid, i.e., a quantity that can be obtained directly from the vibrational density of states. Our present results thus raise the question of whether s_{conf} can indeed be approximated reliably by this difference [24–26].

To advance on this point, we have accurately determined s_{vib} by taking into account the effect of anharmonic vibrations, using two independent approaches. The first one makes use of the idea of Frenkel and Ladd [27–31] of introducing a series of systems which parametrically interpolates between the original system and an Einstein solid, and then carries out a thermodynamic integration to calculate the vibrational entropy of the original system. In practice we have introduced the Hamiltonian $\beta H(\alpha) = \beta H(0) + \alpha \sum_{i=1}^{(1-c)N} |\mathbf{r}_i - \mathbf{r}_{0i}|^2$, where $H(0)$ is the original Hamiltonian, $\beta = 1/T$, α is a spring constant, and $\mathbf{r}_{0i}$ is the equilibrium configuration of the particle i in the original system. We then measure the MSD $\Delta_\alpha = \sum_{i=1}^{(1-c)N} \times [\langle|\mathbf{r}_i - \mathbf{r}_{0i}|^2\rangle]/(1-c)N$, from which we obtain the entropy

$$s_{\mathrm{FL}} = s_{\mathrm{E}}(\alpha_{\max}) + \int_0^{\alpha_{\max}} d\alpha \Delta_\alpha, \tag{1}$$

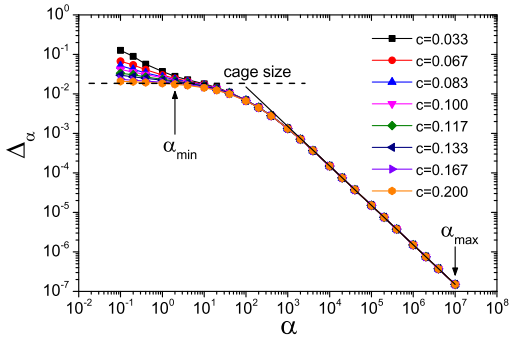

FIG. 2. The mean-squared displacement Δ_α at $T = 0.45$ for $N = 1200$ used for the Frenkel-Ladd thermodynamic integration. The horizontal dashed line is the plateau height for $c = 0.2$ shown in Fig. 1(a). The solid line corresponds to the behavior of the Einstein solid, $\Delta_\alpha = 3/(2\alpha)$.

where $s_E(\alpha_{max})$ is the entropy of the Einstein solid. Figure 2 shows Δ_α for $10^{-1} \leq \alpha \leq 10^7$. For $\alpha > 10^4$, this function follows very closely $3/(2\alpha)$, the behavior of the Einstein solid, and hence we can replace Δ_α with this expression if α is large. The entropy for this Einstein solid is then given by $s_E(\alpha_{max}) = \frac{3}{2} - 3\ln\Lambda - \frac{3}{2}\ln[(\alpha_{max}/\pi)]$, where Λ is the de Broglie thermal wavelength. In practice, we have set $\alpha_{max} = 10^7$.

At small α, the dependence of Δ_α on α becomes weak, suggesting that in this parameter range the particles are vibrating in a cage created by the *original* Hamiltonian and not that of the Einstein solid. However, at the smallest α, Δ_α is not completely flat, since at long times the particles are able to escape slowly from their cages. The height of the plateau in Δ_α allows us to estimate the amplitude of the vibrations in the real system, i.e., to determine the harmonic and anharmonic component of the motion. Indeed, the height of the plateau in Δ_α is consistent with that of $\Delta(t)$ from Fig. 1(a). To estimate the entropy that is due to the vibrational motion, we can evaluate the integral given by Eq. (1) by replacing the contribution to the integral for $\alpha < \alpha_{min} = 2$ with $\alpha_{min}\Delta_{\alpha_{min}}$, thus removing in this manner the contribution of the relaxational part to the entropy. The so-obtained vibrational entropy s_{FL} is shown in Fig. 3(a) (green diamonds). As expected, the c dependence of s_{FL} is smooth and shows no apparent singularity.

The second approach to estimate the anharmonic contribution to the vibrational entropy is to determine the difference between the potential energy of the system and its inherent structure energy, and then to subtract the harmonic part, thus giving the anharmonic part of the vibrational energy [9,32]. One finds that the so-obtained energy is *negative*, which makes it so that the resulting value for the vibrational entropy, $s_{harm} + s_{anh}$, is smaller than s_{harm} [see blue triangles in Fig. 3(a)], a result that agrees with previous studies [9,32]. We see that this quantity agrees very well with our estimate for the vibrational entropy as obtained from the Frenkel-Ladd

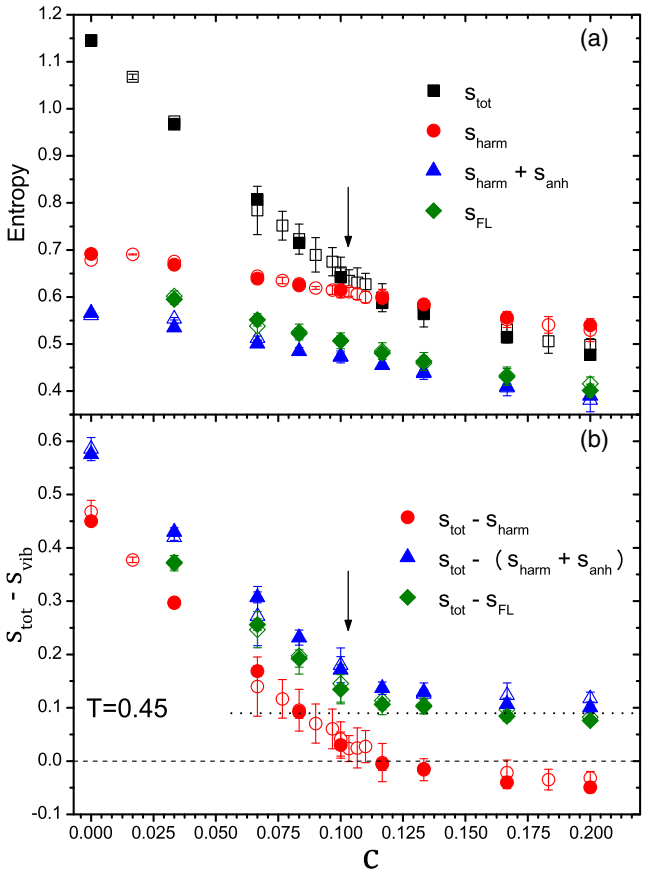

FIG. 3. (a) c dependence of the total entropy s_{tot}, as well as different estimates of the vibrational entropy. (b) c dependence of $s_{tot} - s_{vib}$. The open and filled symbols are for $N = 300$ and $N = 1200$, respectively. The horizontal arrows locate $T_K(c)$, where the skewness of the overlap distribution becomes zero [18].

procedure, indicating that we have determined it with good precision.

Figure 3(b) shows the c dependence of $\Delta s = s_{tot} - s_{vib}$. We see that the improved estimate for s_{vib} makes it so that now Δs no longer goes to zero even at large c. Instead, it shows a kink at the concentration at which the order parameter had a jump [18], indicating that at this point the thermodynamic properties of the system have a singular behavior, i.e., that the phase diagram determined in Ref. [18] is not altered by this improved estimate of s_{vib}. Note that we show data for the two system sizes, and within the accuracy of the data we see no finite size effects.

To determine the origin of the finite value of Δs in the ideal glass phase we probe the potential energy landscape of the system [6–10]. Since at low T the configuration space can be decomposed into the basins of attraction of the inherent structures and vibrations around the ISs, an investigation of the PEL should help us to understand the nature of the motion of the system. Figure 4(a) shows the time dependence of the IS energy $e_{IS}(t)$, [33,34], for 10^4 steps of MC dynamics at $c = 0.2$, a timescale that corresponds to the vibrations inside the cage [see Fig. 1(a)].

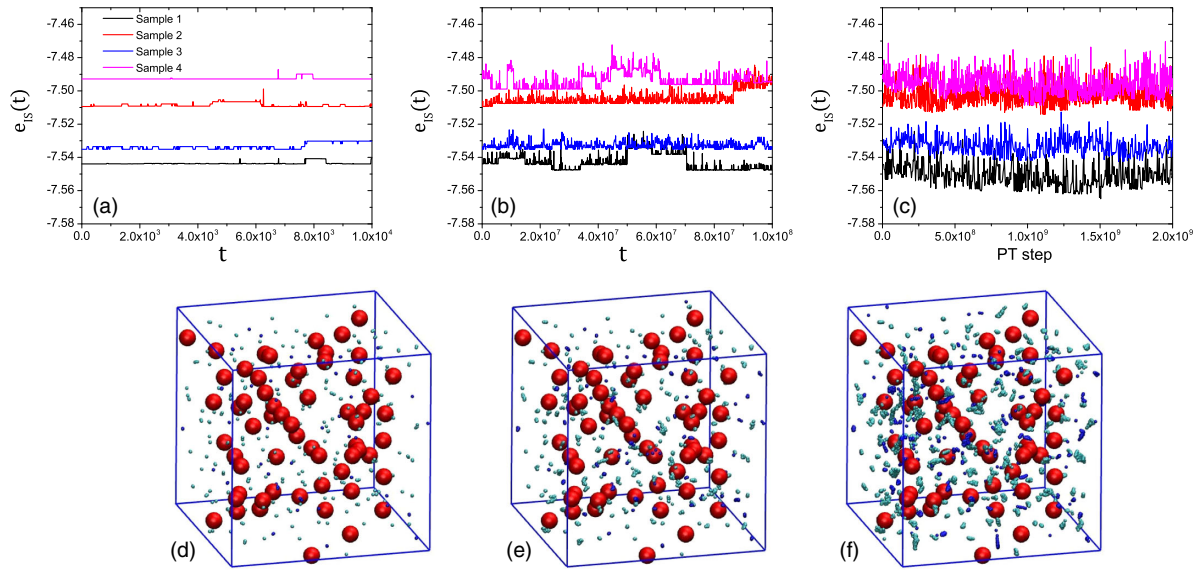

FIG. 4. (a)–(c): $e_{\mathrm{IS}}(t)$ at $T = 0.45$ and $c = 0.2$ for $N = 300$ samples with (a) 10^4 and (b) 10^8 MC time steps, and with (c) 2×10^9 PT time step. Different lines correspond to different samples. (d)–(f): Superposition of the corresponding snapshots (sample 1) of the IS configurations with (d) 10^4 and (e) 10^8 MC time steps, and with (f) 2×10^9 PT time step. Pinned particles are shown in red (reduced in size to 0.5), and nonpinned A and B particles are shown in gray and blue, respectively.

We see that $e_{\mathrm{IS}}(t)$ remains basically constant but shows some spikes, indicating that the system accesses for a short period an excited state before it falls back to the original IS, implying that on this timescale only a single IS is relevant [10]. Figure 4(d) shows the superposition of the configurations for these ISs, and we see that basically all of them are identical, in agreement with the result from Fig. 1(a) that on this timescale the correlation function does not decay. (For the sake of comparison, we show in the Supplemental Material a corresponding plot for the fluid state [23].) If the time window is increased by a factor of 10^4, as in Fig. 4(b), we find that $e_{\mathrm{IS}}(t)$ starts to make larger excursions and that these are no longer reversible, indicating that the system explores new ISs. This is the reason why on this timescale the correlation function decays slightly; see Fig. 1(b). Figure 4(e) shows that now there are indeed many different ISs, but since the corresponding positions of the particles form small clusters, we can conclude that the configurations are quite similar. Finally, we show in Fig. 4(c) the evolution of $e_{\mathrm{IS}}(t)$ as obtained from a PT run. We see that in this case the value of $e_{\mathrm{IS}}(t)$ fluctuates quite significantly, but that these fluctuations are still smaller than the sample-to-sample fluctuations, and therefore we can infer that there are indeed many different ISs even in the equilibrium glass state. This conclusion is corroborated by the real-space image of the configurations, in Fig. 4(f), which now shows quite a few small clusters, i.e., the positions of the particles in the different ISs differ by a small amount. The presence of these different ISs is thus the reason for the finite value of Δs. (We emphasize that the clusters seen in Fig. 4(f) do not depend on the length of the PT run.) In the Supplemental Material [23], we discuss the nature of the motion of the particles for the MC trajectories and show the following: (i) With increasing time, *all* nonpinned particles become diffusive; i.e., they explore the whole available configuration space. (ii) The movement of the particles is often given by a defectlike jump motion or by a back-and-forth jump, but sometimes also involves very complex and compact cooperative rearrangement that involves quite a few particles.

Our results show that the dynamic and thermodynamic properties of a system with pinned particles give a coherent picture of the equilibrium glass state. Although quantities like the self-intermediate scattering function [35–37] or the self–van Hove function (see the Supplemental Material [23]) show decorrelation, the collective functions do not, once the critical pinning concentration is surpassed. At this critical concentration the order parameter shows a jump [18] and the entropy a kink. Our finding that even in the equilibrium glass state particles are able to explore more than one IS indicates that care has to be taken in the definition of the configurational entropy: s_{conf} should not be identified as the difference between the total entropy and the purely vibrational part, since such a definition gives rise to a nonzero s_{conf} even in the ideal glass state. Instead, s_{conf} is related to the number of local free energy minima [38], and for the case of the pinned system such a minimum is a *collection* of ISs that are geometrically close together. The motion of the particles inside this local free energy minimum is the reason for the *partial* relaxation of the collective correlation functions. Although the present study concerns a pinned system, it can be expected that bulk systems have a similar behavior, since local inhomogeneities in the structure will make it so that certain regions in

the very deeply supercooled liquid are already frozen in, thus leading to an extremely high value of the viscosity, whereas other regions are still mobile. So the evoked problem with the correct definition of the configurational entropy is likely to exist also in the case of bulk systems.

We thank G. Biroli, C. Dasgupta, K. Hukushima, Y. Jin, S. Karmakar, and K. Kim for helpful discussions. The numerical simulations were partially performed at the Research Center of Computational Science (RCCS), Okazaki, Japan. W. K. acknowledges Grant No. ANR-15-CE30-0003-02, and A. I. and K. M acknowledge JSPS KAKENHI Grants No. JP16H04034, No. JP17H04853, No. JP25103005, and No. JP25000002.

*Corresponding author.
walter.kob@umontpellier.fr

[1] K. Binder and W. Kob, *Glassy Materials and Disordered Solids: An Introduction to their Statistical Mechanics* (World Scientific, Singapore, 2011).
[2] L. Berthier and G. Biroli, Rev. Mod. Phys. **83**, 587 (2011).
[3] A. Cavagna, Phys. Rep. **476**, 51 (2009).
[4] J. C. Dyre, Rev. Mod. Phys. **78**, 953 (2006).
[5] D. Chandler and J. Garrahan, Annu. Rev. Phys. Chem. **61**, 191 (2010).
[6] M. Goldstein, J. Chem. Phys. **51**, 3728 (1969).
[7] F. H. Stillinger and T. A. Weber, Phys. Rev. A **25**, 978 (1982).
[8] D. Wales, *Energy Landscapes: Applications to Clusters, Biomolecules and Glasses* (Cambridge University Press, Cambridge, 2003).
[9] F. Sciortino, J. Stat. Mech. (2005) P05015.
[10] A. Heuer, J. Phys. Condens. Matter **20**, 373101 (2008).
[11] B. Ruta, Y. Chushkin, G. Monaco, L. Cipelletti, E. Pineda, P. Bruna, V. M. Giordano, and M. Gonzalez-Silveira, Phys. Rev. Lett. **109**, 165701 (2012).
[12] D. Bock, R. Kahlau, B. Micko, B. Pötzschner, G. Schneider, and E. Rössler, J. Chem. Phys. **139**, 064508 (2013).
[13] V. Giordano and B. Ruta, Nat. Commun. **7**, 10344 (2016).
[14] K. Kim, Europhys. Lett. **61**, 790 (2003).
[15] C. Cammarota and G. Biroli, Proc. Natl. Acad. Sci. U.S.A. **109**, 8850 (2012).
[16] L. Berthier and W. Kob, Phys. Rev. E **85**, 011102 (2012).
[17] W. Kob and L. Berthier, Phys. Rev. Lett. **110**, 245702 (2013).
[18] M. Ozawa, W. Kob, A. Ikeda, and K. Miyazaki, Proc. Natl. Acad. Sci. U.S.A. **112**, 6914 (2015).
[19] W. Kob and H. C. Andersen, Phys. Rev. E **51**, 4626 (1995).
[20] K. Hukushima and K. Nemoto, J. Phys. Soc. Jpn. **65**, 1604 (1996).
[21] R. Yamamoto and W. Kob, Phys. Rev. E **61**, 5473 (2000).
[22] L. Berthier and W. Kob, J. Phys. Condens. Matter **19**, 205130 (2007).
[23] See Supplemental Material at http://link.aps.org/supplemental/10.1103/PhysRevLett.121.205501 for additional information on the simulation methods and further numerical results.
[24] F. Sciortino, W. Kob, and P. Tartaglia, Phys. Rev. Lett. **83**, 3214 (1999).
[25] L. Berthier and D. Coslovich, Proc. Natl. Acad. Sci. U.S.A. **111**, 11668 (2014).
[26] G. Johari, J. Chem. Phys. **116**, 2043 (2002).
[27] D. Frenkel and A. J. Ladd, J. Chem. Phys. **81**, 3188 (1984).
[28] B. Coluzzi, M. Mézard, G. Parisi, and P. Verrocchio, J. Chem. Phys. **111**, 9039 (1999).
[29] S. Sastry, J. Phys. Condens. Matter **12**, 6515 (2000).
[30] L. Berthier, P. Charbonneau, D. Coslovich, A. Ninarello, M. Ozawa, and S. Yaida, Proc. Natl. Acad. Sci. U.S.A. **114**, 11356 (2017).
[31] I. Williams, F. Turci, J. E. Hallett, P. Crowther, C. Cammarota, G. Biroli, and C. P. Royall, J. Phys. Condens. Matter **30**, 094003 (2018).
[32] S. Mossa, E. La Nave, H. E. Stanley, C. Donati, F. Sciortino, and P. Tartaglia, Phys. Rev. E **65**, 041205 (2002).
[33] T. B. Schrøder, S. Sastry, J. C. Dyre, and S. C. Glotzer, J. Chem. Phys. **112**, 9834 (2000).
[34] R. A. Denny, D. R. Reichman, and J.-P. Bouchaud, Phys. Rev. Lett. **90**, 025503 (2003).
[35] S. Chakrabarty, S. Karmakar, and C. Dasgupta, Sci. Rep. **5**, 12577 (2015).
[36] S. Chakrabarty, R. Das, S. Karmakar, and C. Dasgupta, J. Chem. Phys. **145**, 034507 (2016).
[37] M. Ozawa, W. Kob, A. Ikeda, and K. Miyazaki, Proc. Natl. Acad. Sci. U.S.A. **112**, E4821 (2015).
[38] G. Biroli and R. Monasson, Europhys. Lett. **50**, 155 (2000).